Curvature-Based Active Region Segmentation for Improved Image Processing of Aspergillus Species

Nur Rodiatul Raudah Mohamed Radzuan[1], Haryati Jaafar[1,*], Farah Nabilah Zabani[1], Fatin Norazima Mohamad Ariff[1], Fatin Nadia Azman Fauzi[1]

[1] Department of Mechatronic Engineering, Faculty of Electrical Engineering and Technology, Universiti Malaysia Perlis, 02600 Arau, Perlis, Malaysia

ARTICLE INFO	ABSTRACT
  	Aspergillus is one of the most ubiquitous of the airborne saprophytic fungi that can withstand various climatic conditions and could cause multiple type of illness. It can be beneficial to humankind and also can be infectious to humans and animals. Direct microscopic is used by trained microscopist as one of the alternatives in identification process to any specimen that suspected of having fungal infection. Confirmation towards identification is often necessary as the structure of *Aspergillus* is complex and dissimilar in each cycle. In addition, the structure of some species of *Aspergillus* are the almost same, which can be incorrectly recognized. In prevention of misidentification, computer-based *Aspergillus* species identification is proposed. The detection process is the earliest and important process hence, this paper proposed an active region-based segmentation method in order to detect the presence of fungi. This method is literally not depending on the gradient or sharp edges of the object and implementing level set function for curve evolution which able to reduce the computational cost. Originally, this function was developed for tracking fluid interfaces but in this study, this function has been applied to fungi database. Two different methods were tested and compared to observe their ability to segment different 80 of *Aspergillus* images which included four species. Experiments conducted have been compared with the baseline technique and the proposed method is outperformed in terms of accuracy, specificity with average of 90% and PSNR value of greater than 40dB. Meanwhile the active contour (snake) was slightly underperformed but well performed particularly in terms of sensitivity with greater than 80% for all the species. Moreover, upon scrutinizing the dice coefficients provided in both tables, it becomes apparent that there is a lack of significant variance in the values, except in the instance of *Aspergillus fumigatus* (active region-based) that which produces a result below 36%.

1. Introduction

In the new bioeconomy era, fungi infections can be acquired either environmentally or endogenously. Some fungi grow in environmental niches as saprophytes and patients can be infected

---

* *Corresponding author.*
E-mail address: haryati@unimap.edu.my

via inhalation of spores easily. Despite thousand species of fungi existed, *Aspergillus* is one of the most ubiquitous of the airborne saprophytic fungi that can be found in various climatic conditions and could cause multiple type of illness from a simple allergic reaction to life-threatening disease [1]. *Aspergillus*'s conidia present in the air and constantly inhaled by humans but normally it is harmless except for people with compromised immune system. However, the individuals with neutropenia, has a cancer or undergo chemotherapy also have high potential to be infected [2]. The recognition of *Aspergillus* species is important in order to help the physicians to proceed with the treatment. Commonly, the trained microscopist will handle all the specimens before handing over all the results related. Yet, this method is rendering some flaws and confirmation is often necessary.

Due to the aforementioned problems, computer method (image recognition/processing field) is proposed in this study as nowadays, image processing is one of the rapidly growing technologies. In order to analyses the microscopic images, there are two main common methods that have always been used in laboratory; by using light microscope or fluorescence microscope. For example, P.Perner *et al.,* [3] employed digital microscopic image by adapting six fungal strains with 1000x magnification to recognize the airborne fungi spores. Ehgartner *et al.,* [4] presented the fast alternative for 450 microscopic images of *Penicillium chrysogenum*. The images were automatically evaluated to identify the hyphal elements which classified into unbranched hyphae, branched hyphae, small clumps, large clumps and pellets. In another study, the automated fluorescence imaging system was used to capture the fluorescence images in order to collect useful information from the samples. Here, 415 samples consisting of infected and non-infected small skin scales were collected and analysed [5].

The implementation of image processing in microscopic image has been widely investigated for various databases. For example, an image segmentation method such as K- mean and fuzzy C-mean clustering were implemented in [6,7] for blood cells segmentation. However, it was found that although these methods are outperformed for those kinds of database but underperformed for *Aspergillus* database. This is because the structure of fungi and blood cells are completely different even though they are classified as microscopic images. The blood cells have a fixed shape while *Aspergillus*' shape may vary and be more complex therefore, these methods are less suitable for this database. Moreover, although the microscopic image has an informative structure of fungi species, the images' quality can be changed over time. The maturity will change from time to time and certainly will form varying structures during the cycle. Because of this, one of the active contour methods which is active region-based segmentation was investigated as the solution to overcome the problem of complexity of structures.

One of the active contour models known as Snake model, is a commonly used segmentation method that relies on energy constraints and forces within an image. It is particularly suitable for analysing dynamic image data or 3D image data, with its primary goal being the extraction of regions, curvatures, or contours within the region of interest. This method plays a crucial role in various applications, including chest CT image analysis [8], glaucoma detection [9], and the identification of abnormalities in lung images [10]. However, it is worth noting that the traditional Snake model has some limitations. It tends to be sensitive to image noise and heavily relies on the image's edges, which can make it less effective in certain scenarios. For instance, it may not perform well with the model proposed by T.F. Chan *et al.,* [11]. This model, as explained, employs the Mumford-Shah functional for segmentation, level set methods, and curve evolution. By minimizing energy-based segmentation, it demonstrates robustness to noise, making it capable of handling a wide range of images without the need for prior denoising. Additionally, this approach can accurately identify object shapes, lines, and open curves, even in cases where the object boundaries are not well-defined.

Due to the ability of this model to segment the desired region without depending on the strong edges, this method has been widely investigated in various studies. Wong *et al.* proposed an enhanced Chan-Vese algorithm model that is helpful to segment 467 Berkeley's colour images dataset images and increase the speed of computational time [12]. Subsequently, Yun *et al.,* [13] improves Chan-vese model by introducing region-scalable fitting energy to segment the synthetic and real images of blood vessels. On the other hand, a Mumford-Shah functional is adapted to detect objects in vector-values image such as RGB and multispectral regardless of its edge and noise [14,15].

The fungi have a complex structure that a lot of work needs to be done during the processing. Snake model required a larger number of iterations that lead to higher time consumption. Therefore, an image segmentation process with different species of *Aspergillus* with active region-based segmentation technique based on level-set function for curve evolution is proposed in this paper. The level set formulation of Chan-Vese is independent of the gradient or edge of the image unlike the previous active contour model known as active contour (snake) technique [16]. The model is developed to solve the segmentation problem that is involved in such a complex region of interest, and it is somehow suitable with the fungi database used in this paper. This method is basically looking for the inside and outside contours thus optimizing the contours beginning from the initial contour set up at the early stage of segmentation [11]. The model is evolving the curvature of the structure by an iterative process and the contour tends to evolve at different rates depending on the complexity of *Aspergillus* species' structures.

2. Methodology

The overall architecture for this paper is illustrated as in Figure 1. The process is divided into three sections which are data collection, image segmentation and the result and evaluation of segmented images.
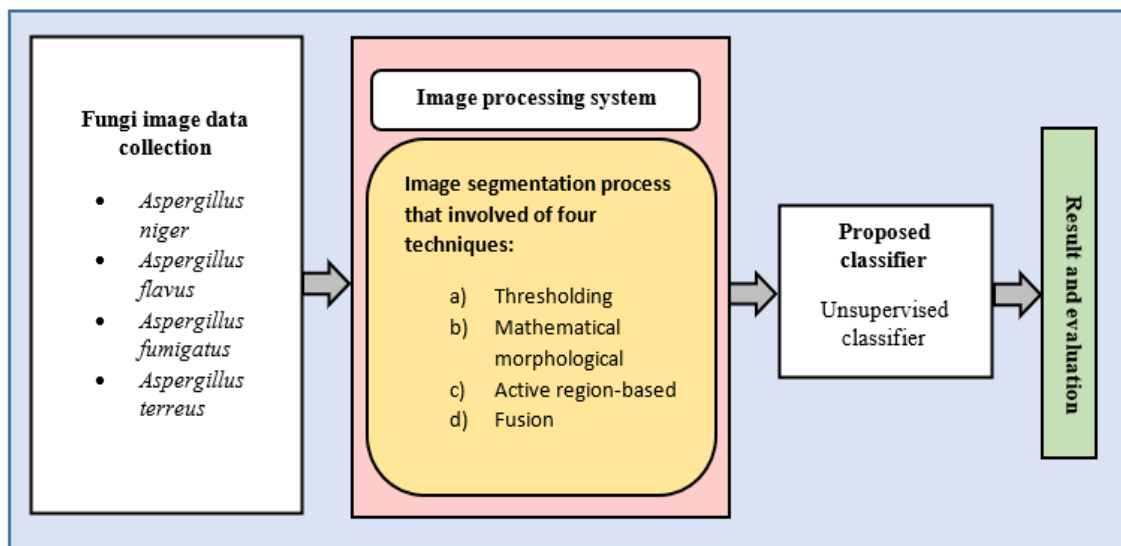

Fig. 1. Overall architecture of proposed method

2.1 Data Acquisition

There are four types of fungi in the current database collection, and they have been used to differentiate each of the morphology. Specimen's collection and preparation were done with guidance by professionals. The fungi samples were provided by the department of microbiology and

parasitology in Hospital Universiti Sains Malaysia (HUSM). The samples were taken from different parts of the patient's body such as saliva, sputum, skin, ear, nail and blood [17]. All patient identification remained confidential. The only revealed information was the type of fungi so that an accurate treatment can be given to patients. Approval for clinical research was deemed unnecessary by the HUSM due to compliance with the patient confidentiality standards set forth. Samples could not be obtained from other resources due to patient confidentiality protection and sample degradation during transport. As a result, 80 images from four commonly found species of *Aspergillus* such as *Aspergillus niger*, *Aspergillus flavus*, *Aspergillus fumigatus* and *Aspergillus terreus* were investigated in this study.
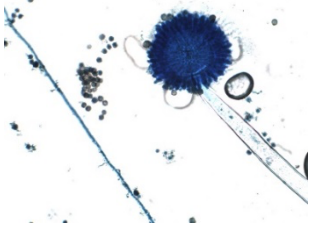
Table 1
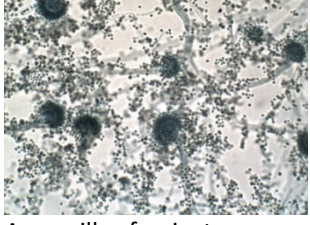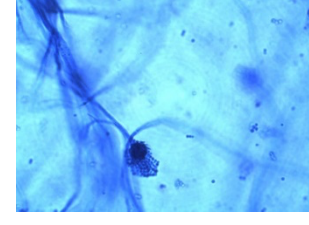Examples of *Aspergillus sp.*
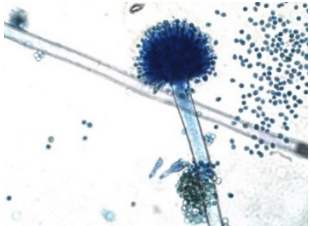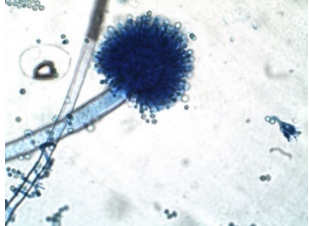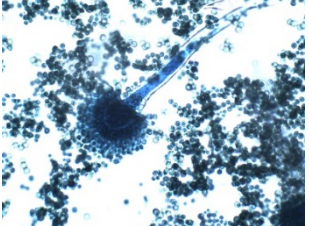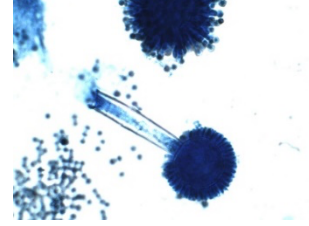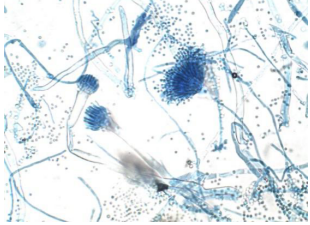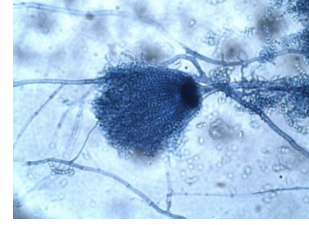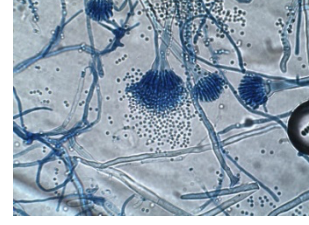
Scientific name and image

Aspergillus flavus

Aspergillus niger

Aspergillus terreus

Aspergillus fumigatus

Table 1 shows different species with different image quality and fungi position. Each species has such a poor quality with unclear characteristics. This explains that most of them are from aging samples which the stain started to fade, or the fungi became too matured (releasing too many spores) thus, affected its original morphological characteristics. Based on Table 1, *Aspergillus fumigatus* presented images from aging slides. The first two images show the fungi is too matured while the other one is an example of immature fungus with unclear image background. Compared to the other

three species, the images in the first row show a greater quality as the shape is more observable and it can be distinguished based on its features. *Aspergillus sp.* has no big difference with each other therefore, a clear image is much needed to carry out this research.

2.2 Image Segmentation

The acquired images were then analysed by using computer-assisted technique which is the main focus in this research. In order to detect the species, morphological components of *Aspergillus* need to be extracted out by segmentation and several steps that are involved in image processing technique as shown in Figure 2 [18,19].
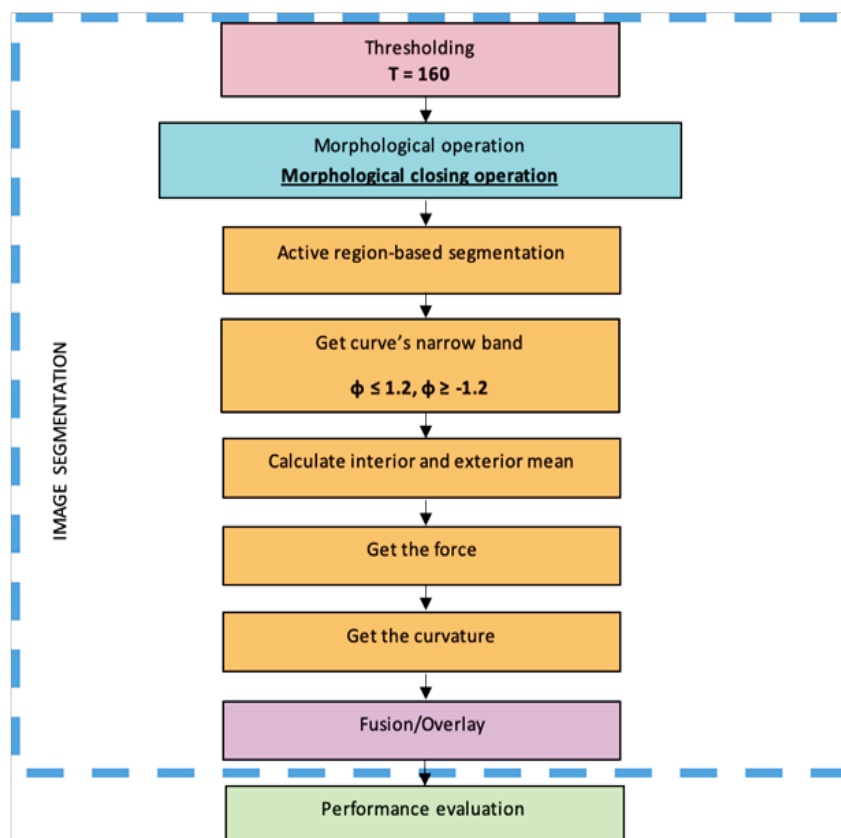

Fig. 2. The implementation steps in microscopic image processing

2.2.1 Thresholding

The purpose of this technique is to distinguish the foreground and background of an input image so that the region of interest (ROI) can be segmented out. The input image was defined as $X \in R^{H \times W}$ with the dimension of $H \times W$ pixels. The coloured X image was converted into a grayscale image. Range values of threshold from 50 to 180 were manually adjusted to determine the optimal value that can produce clearer image. The result shows threshold value with 160 produces the best results where the structure is visible and observable with minimal noise shown compared to others as in Figure 3.

| (a) | (b) | (c) |
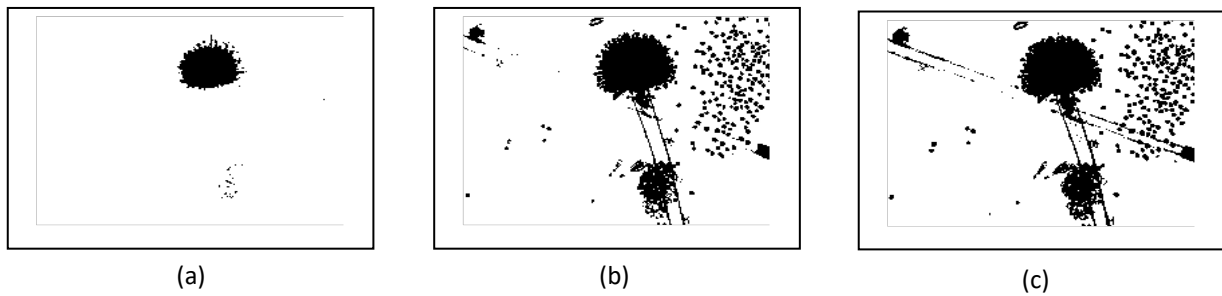
Fig. 3. Image obtained with threshold value (a) 50, the structure of fungus is not fully visible for image recognition. (b) 160, the structure is visible and observable with minimal noise shown. (c) 180, the fungus is visible, but the background noise is also visible which could affect the segmentation process

2.2.2 Morphological operation

Morphological closing operation was performed on the binary image which the process started with dilation followed by erosion. The closing method was the best way in order to fill up small holes and smooth the outline while preserving its shape and size. In addition, some elements that might diminish during thresholding can be restored at this stage so that the object is compact enough and clearly seen. The algorithm of closing operation that used dilation followed by erosion is defined as below [20]. Assume $g\,(i,j)\ =\ G$ and $G\,\bullet\,B\ =\ p\,(i,j)$.

$$G \bullet B = (G \oplus B) \ominus B \tag{1}$$

Where an image G is closing with structural element B. A disk-shaped structural element with a radius of 1 was used in this operation as its shape and size basically fits the subject in the input image. The important small elements that were discarded throughout the thresholding process could be retrieved during this process so that the final segmented image could provide more accurate information. Figure 4 provided fungi images before and after morphological closing operation technique is applied. Only a slight difference can be seen because the radius of structural element used is small but however, during this process it literally affects the quality of the entire image. A mere change can restore the significant features of fungi, especially the upper part of fungus that is surrounded with small conidia. For reference, the difference can be observed in the red circles area.

| (a) | (b) |
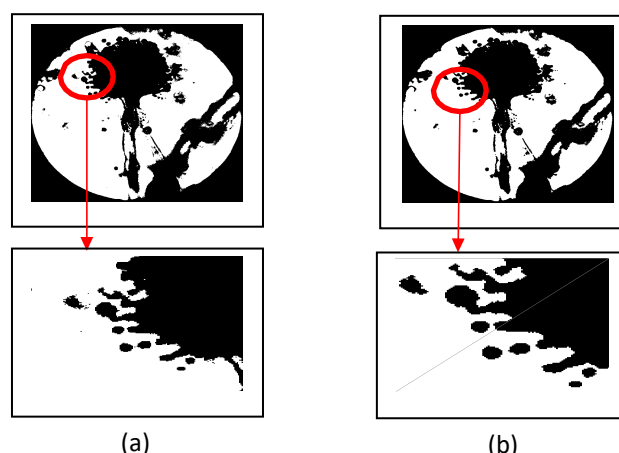
Fig. 4. The image of *Aspergillus fumigatus* (a) is before and (b) is after morphological operation and its enlarged version

2.2.3 Active region-based segmentation

In order to segment out a particular area within the obtained binary image for further analysis, the active region-based segmentation method was implemented. The important particular area that needs to be extracted within the image was the most complex part of *Aspergillus* that contained informative elements of the fungi i.e., conidia, phialides, metulae and vesicle. The process of image segmentation includes four steps as illustrated in Figure 2.

Firstly, narrow band initialization is adapted to compute level set near to the contour and decrease the computational complexity. At this stage, the pixels of the image were remapped, and the rest of unwanted pixels were removed according to the range that has been set up. For this part, $Z = 1.2 \leq \varphi \geq -1.2$ of narrow band has been used to build a boundary near the edge. The remapping process is only involved in the area with desired region and the rest unwanted pixels were discarded to reduce complexity and accelerate the computation. To achieve this goal, sliding neighbourhood operation has been used [21,22]. The remaining pixels were compact with important information for later use. Figure 6 shows an example of the sliding neighbourhood operation. An image with a size of 10×7 pixels was divided into 3×3 pixels block of window neighbourhood as shown in Figure 6 (a). According to Figure 6 (b), the 10×7 matrix was rearranged into 70 columns of temporary matrix ($10 \times 7 = 70$) and each column has nine rows of pixel, presenting ($3 \times 3 = 9$) window. Then, to reduce the temporary matrix, local mean technique M_i was used.

$$M_i = \frac{1}{N}\sum_{j=1}^{n} \omega_j \tag{2}$$

Where ω is the size of window neighbourhood, j is number of pixels in each neighbourhood, i the number of columns and N is the total number of pixel block presented. After each local mean determined, the temporary matrix remapping into single row of matrix and rearranged again into its original shape as displayed in Figure 6 (c) and (d).

Secondly, the energy minimization-based segmentation is employed. The basic idea of this concept is the fitting term will reach minimization (Fitting = 0) once the curve is on the boundary of object. The equation involved for this concept is provided as in Eq. (3) [23,24]. Assume $z(i,j) = u_o$ and $F1(C) + F2(C) = f(i,j)$.

$$F1(C) + F2(C) = \int_{inside\ (C)} |u_0 - c1|^2\, dx\, dy + \int_{outside\ (C)} |u_0 - c2|^2\ dx\, dy \tag{3}$$

Eq. (3) has two forces that represent in terms of $F1$ and $F2$. The first term is the force to shrink the contour while the other term is to expand the contours (C). $c1$ and $c2$ here is interpreted as the mean of inside and outside of the contour and u_o stands for entire image that formed by two regions of piecewise-constant intensities. Both forces are balance when the curve is completely reaches the exact boundary. Additionally, Figure 5 exemplify some different cases on how basic fitting term for region detection is occur in an image.
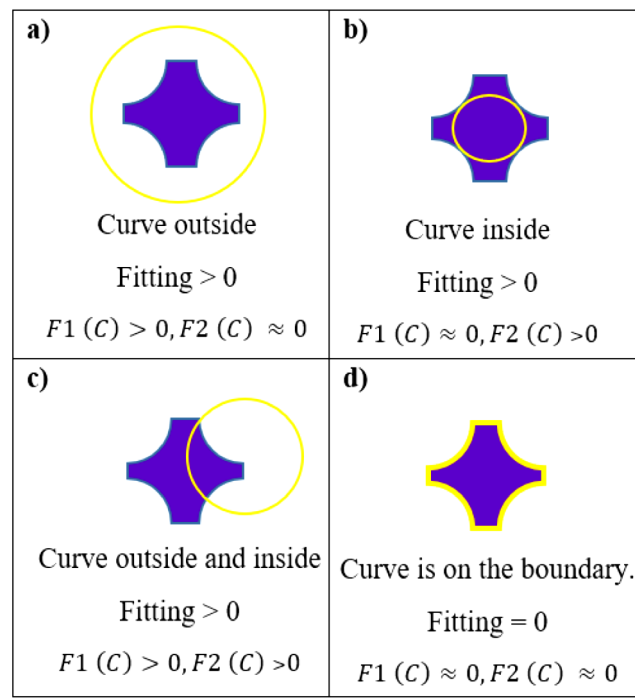
Fig. 5. Position of the curve and its fitting term

Next, the level set representation and motion by mean curvature by Osher and Sethian [25] been used expansively as it allows for cusps, merging, breaking as well as automatic topology changes. The evolving curve is defined as $C = \{(x, y)|\phi(x, y) = 0\}$ where C is an open boundary and normal $L = \frac{\nabla_\varphi}{|\nabla_\varphi|}|$. In addition, level set function can be multiple and allow for triple junctions or complex and vague topologies. For a better description, Table 2 provided a few examples of how level set function is performing by representing 2^n phases or segment [26]. n is defined as $\varphi = (\varphi), \ldots. \varphi')$ and it concludes that the greater the level set n, the greater the number of regions.
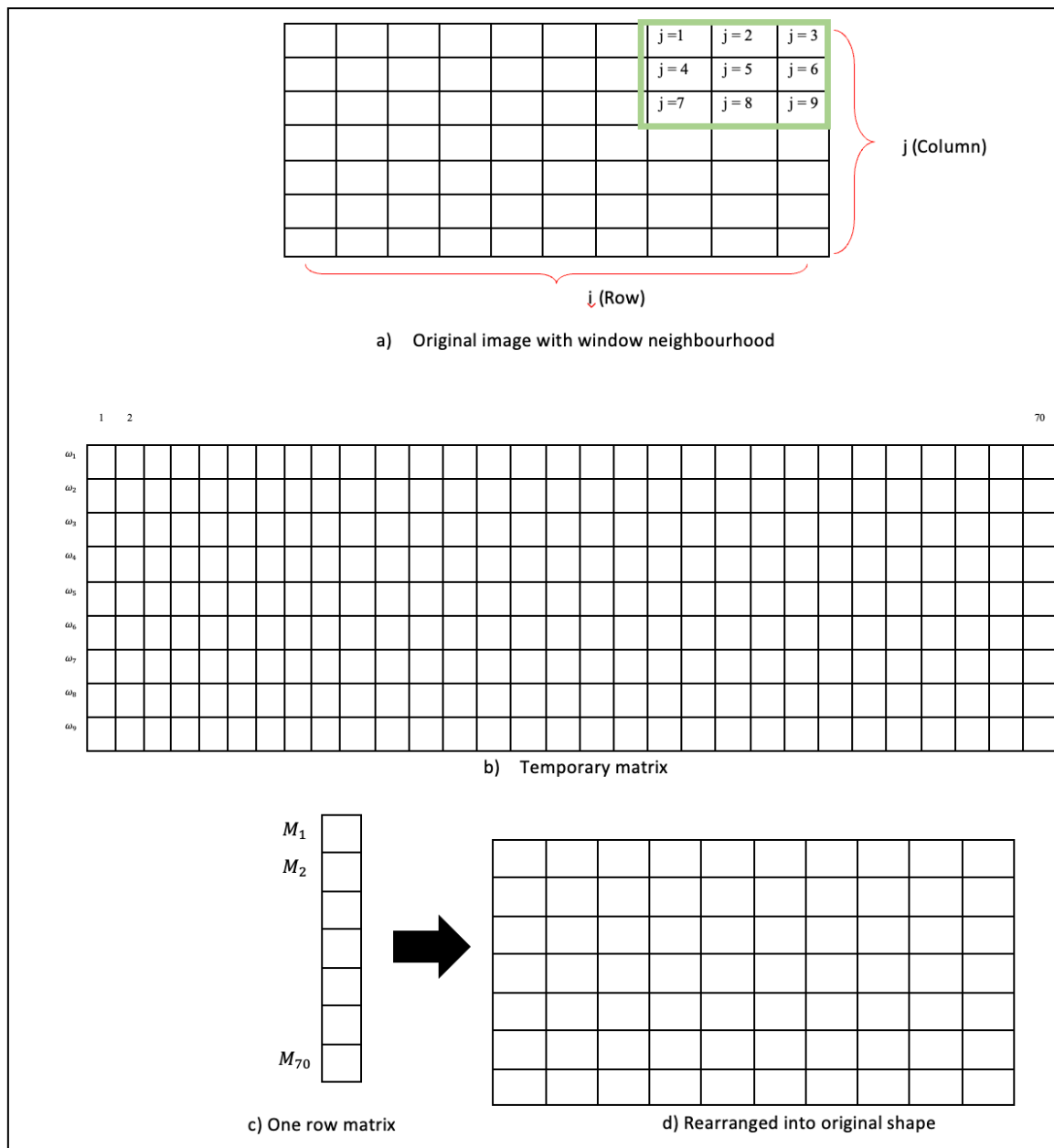
Fig. 6. Remapping of pixel after getting the narrow band by using sliding neighbourhood operation
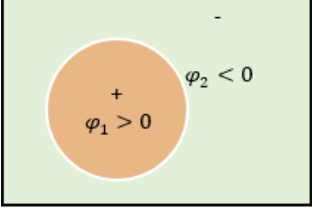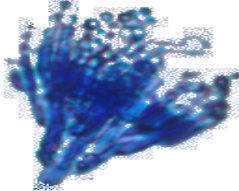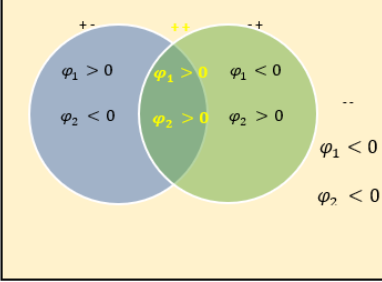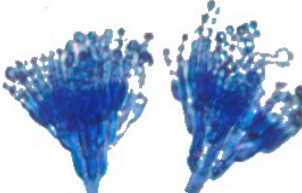
2.2.4 Fusion

After segmentation process was completely done, the image obtained that displayed as binary image been fused with the original image (RGB image). This fusion was made to get the final result as coloured image, in line with the main aim of this section; segmentation of colour image [27,28]. Plus, imposed binary image on RGB image also help to make sure the particular area was cropping out nicely while preserved the features of *Aspergillus sp*. Below shows the algorithm for this process. Let assume image $K = k(i)$.

$$k(i) = x(i) \cap y(i) \tag{4}$$

Where $k(i)$ is the result image, $x(i)$ is the input image and $y(i)$ is the segmented binary image.

Table 2
Multiple level set representations and partitions

Level set and phase	Explanation and Result
1 level set function 2 phase segmentation	Curve $\{\varphi = 0\}$ A curve given by $\varphi_1 = 0$ and $\varphi_2 = 0$ The domain is divided into two regions: $\{\varphi_1 > 0, \varphi_2 > 0\}, \{\varphi_1 > 0, \varphi_2 < 0\}$ This is the result of a single curve evolving a single region of *Aspergillus fumigatus.* The curve has fit in the boundary of the structure and segmented out only a single subject and discarded the rest of the subject.
2 level set functions 4 phase segmentation	Curve $\{\varphi_1 = 0\} \cup \{\varphi_2 = 0\}$ Two curves given by $\varphi_1 = 0$ and $\varphi_2 = 0$. The domain is divided into four regions: $\{\varphi_1 > 0, \varphi_2 > 0\}, \{\varphi_1 > 0, \varphi_2 < 0\}, \{\varphi_1 < 0, \varphi_2 > 0\},$ $\{\varphi_1 < 0, \varphi_2 < 0\}$ Two curves stated are representing two sets of *Aspergillus fumigatus.* Based on the result obtained above, a single curve was successfully bound onto the boundary of the structures regardless of the position. The background has cropped out and only desired regions presented for further examination.

3 level set functions 8 phase segmentation	Curve $\{\varphi_1 = 0\} \cup \{\varphi_2 = 0\} \cup \{\varphi_3 = 0\}$
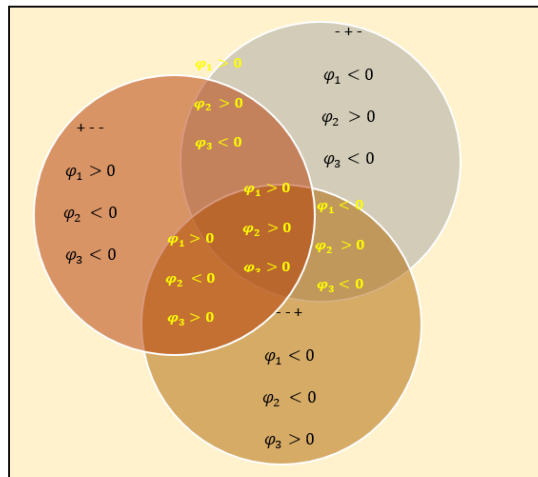
Three curves given by $\varphi_1 = 0, \varphi_2 = 0$ and $\varphi_3 = 0$.
The domain is divided into eight regions:
$\{\varphi_1 > 0, \varphi_2 > 0, \varphi_3 > 0\}, \{\varphi_1 > 0, \varphi_2 > 0, \varphi_3 < 0\},$
$\{\varphi_1 > 0, \varphi_2 < 0, \varphi_3 > 0\}, \{\varphi_1 > 0, \varphi_2 < 0, \varphi_3 < 0\},$
$\{\varphi_1 < 0, \varphi_2 > 0, \varphi_3 > 0\}, \{\varphi_1 < 0, \varphi_2 > 0, \varphi_3 < 0\},$
$\{\varphi_1 < 0, \varphi_2 < 0, \varphi_3 > 0, \{\varphi_1 < 0, \varphi_2 < 0, \varphi_3 < 0\}\}$

Despite the low-quality image, the whole structure of fungi contained in a single image were successfully segmented out even with different geometrical positions and overlapping to each other. Different from the other two images, this image is focusing on cropping out the full structure of *Aspergillus fumigatus* which includes the upper and lower part of it.
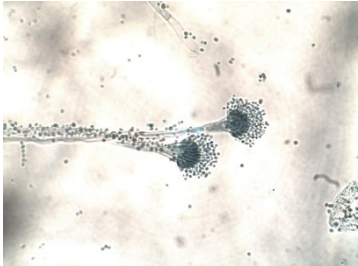
3. Results
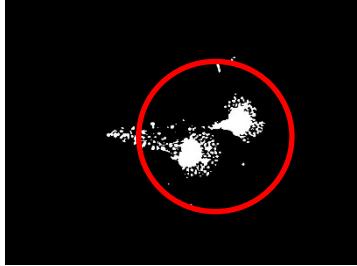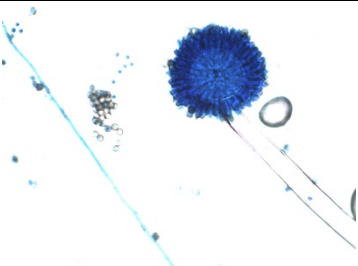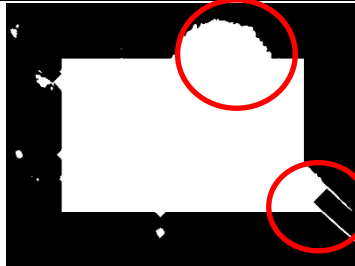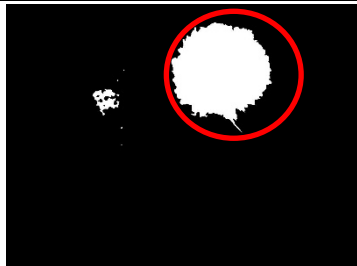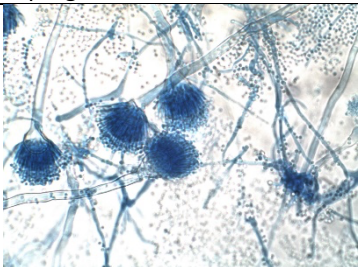
In this paper the performance evaluation is presented into subjective and objective evaluations. Subjective evaluation is visually observed by human while objective evaluation used an algorithm to measure the images' quality. Four species of *Aspergillus* with two positions of each species been tested and evaluated. The experiments have been implemented in Matlab R2018 (b) and have been tested in Intel Core i7, 2.1GHz CPU, 8G RAM and the Windows 10 operating system.

3.1 Performance Evaluation Based on Subjective Evaluation

The evaluations have been made by comparing the performances of snake and active region-based segmentation techniques. For fair comparison, both techniques are used the same number of iterations which are 1300. Table 3 shows the comparison of image segmentation for *Aspergillus* species based on active contour (snake) and active region-based techniques. Based on this table, active contour (snake) was not able to crop out the whole structure as active region-based did. 1300

number of iterations is adequate enough for the proposed method but not for active contour (snake) technique. More iteration numbers are needed in order to fully crop out the desired region which could affect the time consumption. As for active region-based segmentation, fully structure of *Aspergillus flavus* can be seen and it able to remove the undesirable noise in the background.

Table 3
Segmented images of A*spergillus sp.*

Original image	Active contour (Snake)	Active region-based
Aspergillus flavus		

| Aspergillus fumigatus | | |

| Aspergillus niger | | |

| Aspergillus terreus | | |

3.2 Performance Evaluation Based on Objective Evaluation

Table 4 and Figure 7 show the mean of accuracy, sensitivity and specificity obtained by implementing active region-based technique while Table 5 and Figure 8 are the overall means attained from the second technique which is active contour (snake). Accuracy, sensitivity, specificity and dice coefficient are assessed using a pair of images, with one serving as the ground truth reference [29]. The values for these metrics are then calculated using the following equations.

$$accuracy = \frac{TP+TN}{FN+FP+TP+TN} \tag{5}$$

$$sensitivity = \frac{TP}{TP+FN} \tag{6}$$

$$specificity = \frac{TN}{TN+FP} \tag{7}$$

$$Dice\ Coefficient = \frac{2TP}{2TP+FP+FN} \tag{8}$$

where TP, TN, FP, FN denote true positive, true negative, false positive and false negative that can be predicted from segmented images.

Based on Table 4 and Figure 7, *Aspergillus niger* has the greatest mean of accuracy, sensitivity and dice coefficient with 98.53%, 98.29% and 91.84% respectively while for active contour (snake), *Aspergillus fumigatus* recorded the highest ones with 97.37% and 97.92%. *Aspergillus fumigatus* also achieved a notably higher dice coefficient value compared to the other species, registering an impressive 98.61%. This can be attributed to the striking similarity between the benchmark images and the ones being compared, resulting in a substantial number of true positive pixel matches. Besides that, in terms of specificity, the highest value recorded for active region-based is *Aspergillus terreus* with 99.16% and *Aspergillus niger* for active contour (snake) with 98.39%.

Table 4
Mean of accuracy, sensitivity and specificity for active region-based technique

Species	Accuracy	Sensitivity	Specificity	Dice Coefficient
Asp. flavus	97.36	83.91	99.15	81.12
Asp. fumigatus	94.55	38.63	96.67	35.21
Asp. niger	**98.53**	**98.29**	98.55	**91.84**
Asp. terreus	95.78	69.40	**99.16**	78.47

The mean of sensitivity and specificity presented in Table 4 and Table 5 have a huge different between each species. Referring to Table 4 which implemented active region-based technique, the lowest mean of sensitivity calculated is *Aspergillus fumigatus* with only 38.63% followed by *Aspergillus terreus* and *Aspergillus flavus* with 69.40% and 83.91% respectively. For mean of specificity in Table 5 and Figure 8, *Aspergillus fumigatus* also has the lowest value which is 51.52% followed with *Aspergillus terreus*, *Aspergillus flavus* and *Aspergillus niger*. Both techniques are eligible for segmenting however, the results presented are different to each other. Furthermore, when examining the dice coefficients presented in both tables, it becomes evident that there is not a significant difference between the values, except in the case of *Aspergillus fumigatus*. In this instance, the dice coefficient obtained through the active region-based method is considerably lower compared to the Snake model. However, it is important to note that despite the promising dice coefficient value obtained for *Aspergillus fumigatus* using the Snake model, the subjective evaluation yielded contrasting results, as shown in Table 3.
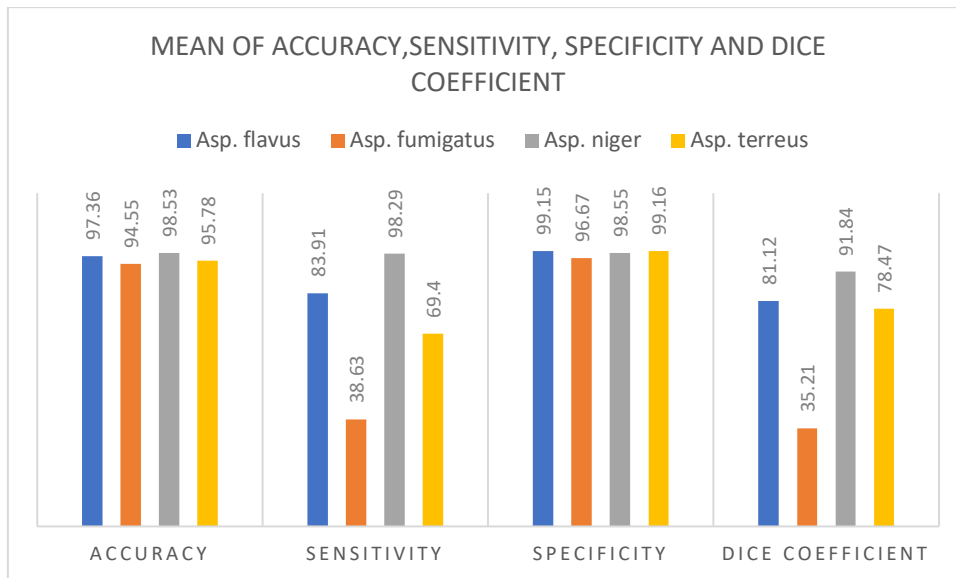
Fig. 7. Comparison of mean for active region-based technique

Next, after analysing the data presented in both Table 4 and Table 5, it is apparent that there is only a slight variance in accuracy values between the two methods. Nonetheless, the proposed technique exhibits superior performance when compared to the active contour (snake) method. Regarding sensitivity, the active region-based technique falls short in comparison to active contour (snake), while the reverse holds true for specificity. Notably, *Aspergillus fumigatus* and *Aspergillus terreus* both exhibit lower values compared to other species. This can be attributed to various factors, including structural complexity, the aging of slides, and variations in image intensity.

Table 5
Mean of accuracy, sensitivity and specificity for active contour
(snake) technique

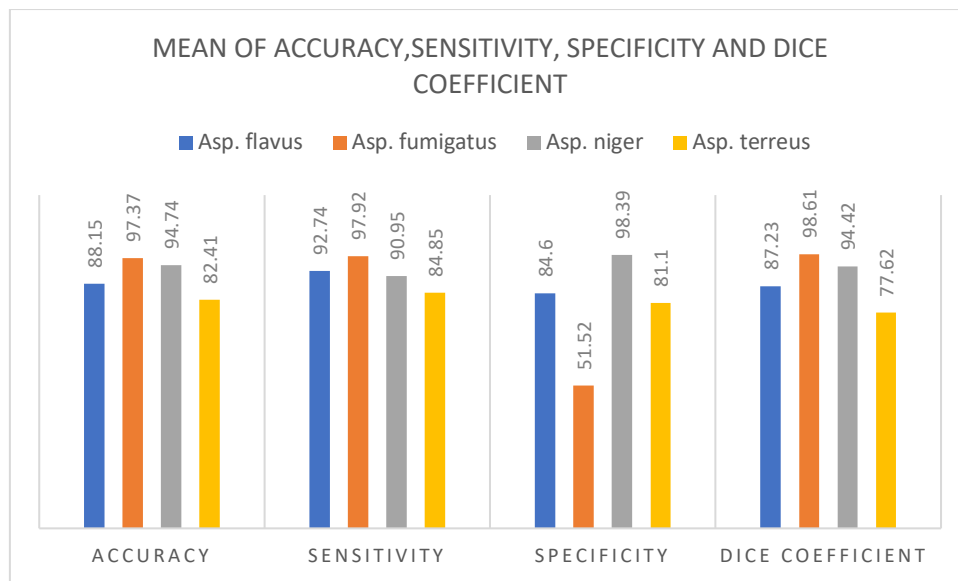| Species	Accuracy	Sensitivity	Specificity	Dice Coefficient
Asp. flavus	88.15	92.74	84.60	87.23
Asp. fumigatus	**97.37**	**97.92**	51.52	**98.61**
Asp. niger	94.74	90.95	**98.39**	94.42
Asp. terreus	82.41	84.85	81.10	77.62

Fig. 8. Comparison of mean for active contour (snake) technique

In addition, Table 6 and Figure 9 present the mean of PSNR values for all the species included in this research by implementing both active region-based and active contour (snake) techniques. PSNR and MSE serve as objective metrics to evaluate the quality and fidelity of images when compared to a reference image. PSNR focuses on providing a perceptually meaningful signal-to-noise ratio, while MSE directly measures the average error between pixel values. Higher PSNR values indicate lower levels of distortion and better image quality while lower MSE values imply a smaller amount of error and closer similarity to the reference image. Both evaluations are calculated by using equations as follows [30].

$$PSNR = 10 \, log_{10} \left(\frac{S^2}{MSE} \right) \tag{9}$$

where R is the maximum fluctuation existed in input image data type and MSE is the mean squared error which is defined as

$$MSE = \frac{1}{N} \sum_{M,N} [I_1(i,j) - I_2(i,j)]^2 \tag{10}$$

By observing the values recorded in Table 6 and Figure 9, the highest mean of PSNR value for active region-based technique is *Aspergillus niger* with 53.30 dB. The value is increasing from *Aspergillus flavus* to *Aspergillus niger* but decrease sharply for *Aspergillus terreus* with only 38.83 dB. Compared to active contour (snake), *Aspergillus fumigatus* has higher PSNR value with 41.00 dB regardless of its vague image and followed by *Aspergillus flavus*, *Aspergillus niger* and the least one is *Aspergillus terreus*. The values presented for active contour snake only slightly different to each other and not constantly increasing. Based on the highest values obtained by using these two techniques, active region-based technique is outstanding compared to the active contour (snake). This shows that, the image produced by implementing active region-based technique is better than active contour snake in term of its quality as the greater the number of PSNR, the finer the image.

Table 6
Comparison means of PSNR for both techniques of *Aspergillus sp*

Species	Active region-based (dB)	Active contour (snake) (dB)
Asp. flavus	40.80	38.91
Asp. fumigatus	42.58	**41.00**
Asp. niger	**53.30**	38.02
Asp. terreus	38.83	37.13
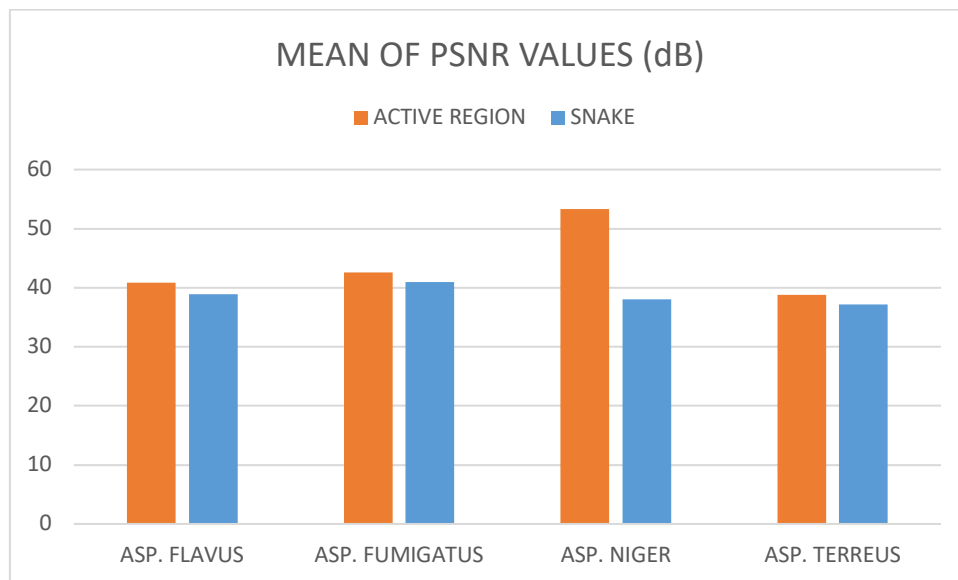
Fig. 9. The comparison for PSNR mean values

4. Conclusions

A comparative study of active region-based and active contour (snake) techniques is conducted in order to observe its capability to segment the *Aspergillus* images. In this study, the original images went through several processes such as thresholding and morphological operation to convert the image to binary image before proceeding with segmentation and fusion processes. The database then being assessed and the performance evaluations (subjective and objective) were presented in Section 3 together with thorough explanation in each subchapter. The objective evaluations were assessed in term of accuracy, sensitivity, specificity, dice coefficient and PSNR values to indicate the best segmentation technique for this kind of database. Based on the accuracy, specificity and PSNR values, the proposed method has a better outcome compared to the active contour (snake). The accuracy and specificity values obtained were greater than 94% and PSNR values were in range of 35db to 55dB. Meanwhile, active contour (snake) is outperformed in term of sensitivity value with higher than 90%. The higher the value obtained, the greater the quality of the segmented image. However, the values obtained in each category for both techniques are only slightly different to each other as the active contour (snake) technique still produce 50% to 98% of accuracy and specificity. Moreover, when considering the dice coefficient, both methods have consistently achieved values ranging from 76% to 99% for all the species, with the exception of *Aspergillus fumigatus* (active region-based), which yielded only 35.21%. Nevertheless, despite the higher dice coefficient obtained from the active contour (snake) model, the final segmented image fails to accurately represent the structure of *Aspergillus*, as highlighted in Table 3. Lastly, based on subjective evaluation, the active contour (snake) technique still can segment the image but the final outcome is not achieving the gold standard of this study. Though the proposed method is produced a better and more observable final

image, it is still lacking in some ways for instance, it consumed a lot of time and need a huge number of iterations.

Acknowledgement

References

[1] Mousavi, Bita, Mohammad T. Hedayati, Newsha Hedayati, Macit Ilkit, and Seyedmojtaba Syedmousavi. "Aspergillus species in indoor environments and their possible occupational and public health hazards." *Current medical mycology* 2, no. 1 (2016): 36. https://doi.org/10.18869/acadpub.cmm.2.1.36

[2] Larone, Davise Honig, and Davise Honig Larone. *Medically important fungi: a guide to identification*. Vol. 196. New York: Elsevier, 1987.

[3] Perner, Petra, Horst Perner, Silke Janichen, and Angela Buhring. "Recognition of airborne fungi spores in digital microscopic images." In *Proceedings of the 17th International Conference on Pattern Recognition, 2004. ICPR 2004.*, vol. 3, pp. 566-569. IEEE, 2004. https://doi.org/10.1109/ICPR.2004.1334592

[4] Ehgartner, Daniela, Christoph Herwig, and Jens Fricke. "Morphological analysis of the filamentous fungus Penicillium chrysogenum using flow cytometry—the fast alternative to microscopic image analysis." *Applied Microbiology and Biotechnology* 101 (2017): 7675-7688. https://doi.org/10.1007/s00253-017-8475-2

[5] Mäder, Ulf, Niko Quiskamp, Sören Wildenhain, Thomas Schmidts, Peter Mayser, Frank Runkel, and Martin Fiebich. "Image-processing scheme to detect superficial fungal infections of the skin." *Computational and mathematical methods in medicine* 2015 (2015). https://doi.org/10.1155/2015/851014

[6] Viswanathan, P. "Fuzzy C means detection of leukemia based on morphological contour segmentation." *Procedia Computer Science* 58 (2015): 84-90. https://doi.org/10.1016/j.procs.2015.08.017

[7] Kumar, Sachin, Sumita Mishra, Pallavi Asthana, and Pragya. "Automated detection of acute leukemia using k-mean clustering algorithm." In *Advances in Computer and Computational Sciences: Proceedings of ICCCCS 2016, Volume 2*, pp. 655-670. Springer Singapore, 2018. https://doi.org/10.1007/978-981-10-3773-3_64

[8] Rakesh, Spoorthi, and Shanthi Mahesh. "Nodule segmentation of lung CT image for medical applications." *Global Transitions Proceedings* 2, no. 1 (2021): 80-83. https://doi.org/10.1016/j.gltp.2021.01.011

[9] Zulfira, Fakhira Zahra, Suyanto Suyanto, and Anindita Septiarini. "Segmentation technique and dynamic ensemble selection to enhance glaucoma severity detection." *Computers in Biology and Medicine* 139 (2021): 104951. https://doi.org/10.1016/j.compbiomed.2021.104951

[10] Parhar, Sudhanshu, Arpan Roy, Kundan Kumar, Ashwini Kumar, and Gouri Shankar Mishra. "Lung Field Segmentation of X-ray Images by Normalized Gradient Gaussian Filter and Snake Segmentation." In *2021 2nd International Conference for Emerging Technology (INCET)*, pp. 1-5. IEEE, 2021. https://doi.org/10.1109/INCET51464.2021.9456146

[11] Chan, Tony F., and Luminita A. Vese. "Active contours without edges." *IEEE Transactions on image processing* 10, no. 2 (2001): 266-277. https://doi.org/10.1109/83.902291

[12] Wong, Ooi Qun, and Parvathy Rajendran. "Image segmentation using modified region-based active contour model." *J. Eng. Appl. Sci* 14 (2019): 5710-5718. https://doi.org/10.36478/jeasci.2019.5710.5718

[13] Tian, Yun, Ming-quan Zhou, Zhong-ke Wu, and Xing-ce Wang. "A region-based active contour model for image segmentation." In *2009 International Conference on Computational Intelligence and Security*, vol. 1, pp. 376-380. IEEE, 2009. https://doi.org/10.1109/CIS.2009.238

[14] Chan, Tony F., B. Yezrielev Sandberg, and Luminita A. Vese. "Active contours without edges for vector-valued images." *Journal of Visual Communication and Image Representation* 11, no. 2 (2000): 130-141. https://doi.org/10.1006/jvci.1999.0442

[15] Mumford, David Bryant, and Jayant Shah. "Optimal approximations by piecewise smooth functions and associated variational problems." *Communications on pure and applied mathematics* (1989). https://doi.org/10.1002/cpa.3160420503

[16] Hemalatha, R., T. Thamizhvani, A. Josephin Arockia Dhivya, Josline Elsa Joseph, Bincy Babu, and R. Chandrasekaran. "Active contour based segmentation techniques for medical image analysis." *Medical and Biological Image Analysis* 4, no. 17 (2018): 2. https://doi.org/10.5772/intechopen.74576

[17] Singh, Gurjeet, and A. D. Urhekar. "Virulence factors detection in Aspergillus isolates from clinical and environmental samples." *Journal of clinical and diagnostic research: JCDR* 11, no. 7 (2017): DC13.

[18] Radzuan, Nur Rodiatul Raudah Mohamed, Haryati Jaafar, and Farah Nabilah Zabani. "An Application of Principal Component Analysis in Aspergillus Species Identification." In *2022 IEEE 10th Conference on Systems, Process & Control (ICSPC)*, pp. 296-301. IEEE, 2022. https://doi.org/10.1109/ICSPC55597.2022.10001780

[19] Radzuan, Nur Rodiatul Raudah binti Mohamed, Haryati Binti Jaafar, and Aimi Salihah Binti Abdul Nasir. "An Identification of Aspergillus Species: A Comparison on Supervised Classification Methods." In *Proceedings of the 12th National Technical Seminar on Unmanned System Technology 2020: NUSYS'20*, pp. 965-977. Springer Singapore, 2022. https://doi.org/10.1007/978-981-16-2406-3_71

[20] Sonka, Milan, Vaclav Hlavac, and Roger Boyle. *Image processing, analysis and machine vision*. Springer, 2013.

[21] Czyżniewski, Mateusz, Rafał Łangowski, Dawid Klassa, and Mateusz Matwiszyn. "A case study of robust sliding mode control applied to inverted pendulum on a cart." In *2021 25th International Conference on Methods and Models in Automation and Robotics (MMAR)*, pp. 156-161. IEEE, 2021. https://doi.org/10.1109/MMAR49549.2021.9528458

[22] Jaafar, Haryati, Salwani Ibrahim, and Dzati Athiar Ramli. "A robust and fast computation touchless palm print recognition system using LHEAT and the IFkNCN classifier." *Computational intelligence and neuroscience* 2015 (2015): 43-43. https://doi.org/10.1155/2015/360217

[23] Getreuer, Pascal. "Chan-vese segmentation." *Image Processing On Line* 2 (2012): 214-224. https://doi.org/10.5201/ipol.2012.g-cv

[24] Thanh, Dang NH, Nguyen Ngoc Hien, V. B. Surya Prasath, Le Thi Thanh, and Nguyen Hoang Hai. "Automatic initial boundary generation methods based on edge detectors for the level set function of the Chan-Vese segmentation model and applications in biomedical image processing." In *Frontiers in Intelligent Computing: Theory and Applications: Proceedings of the 7th International Conference on FICTA (2018), Volume 2*, pp. 171-181. Springer Singapore, 2020. https://doi.org/10.1007/978-981-13-9920-6_18

[25] Osher, Stanley, and James A. Sethian. "Fronts propagating with curvature-dependent speed: Algorithms based on Hamilton-Jacobi formulations." *Journal of computational physics* 79, no. 1 (1988): 12-49. https://doi.org/10.1016/0021-9991(88)90002-2

[26] Jiang, Jian-Guo, Yanrong Guo, Shu Zhan, and Hong Li. "Segmentation of knee joints based on improved multiphase Chan-Vese model." In *2008 2nd International Conference on Bioinformatics and Biomedical Engineering*, pp. 2418-2422. IEEE, 2008. https://doi.org/10.1109/ICBBE.2008.937

[27] Radzuan, Nur Rodiatul Raudah Mohamed, Haryati Jaafar, Farah Nabilah Zabani, and Aimi Salihah Abdul Nasir. "An improvement of morphological operation and active region based segmentation in image enhancement and segmentation for Aspergillus species." In *2019 IEEE 9th International Conference on System Engineering and Technology (ICSET)*, pp. 241-246. IEEE, 2019. https://doi.org/10.1109/ICSEngT.2019.8906363

[28] Ghani, Ahmad Shahrizan Abdul. "Image contrast enhancement using an integration of recursive-overlapped contrast limited adaptive histogram specification and dual-image wavelet fusion for the high visibility of deep underwater image." *Ocean Engineering* 162 (2018): 224-238. https://doi.org/10.1016/j.oceaneng.2018.05.027

[29] Kumar, Ankit, Sudeb Majee, and Subit K. Jain. "CDM: A coupled deformable model for image segmentation with speckle noise and severe intensity inhomogeneity." *Chaos, Solitons & Fractals* 172 (2023): 113551. https://doi.org/10.1016/j.chaos.2023.113551

[30] Setiadi, De Rosal Igantius Moses. "PSNR vs SSIM: imperceptibility quality assessment for image steganography." *Multimedia Tools and Applications* 80, no. 6 (2021): 8423-8444. https://doi.org/10.1007/s11042-020-10035-z